N.A.S.A. NASW-2877

29506-6002-RU-00

ENERGIES OF BACKSTREAMING PROTONS IN THE FORESHOCK

Eugene W. Greenstadt
Space Sciences Department

May 1976

Short Title

ENERGIES OF FORESHOCK PROTONS

Space Sciences Department
TRW Defense and Space Systems Group
One Space Park
Redondo Beach, California 90278

ABSTRACT

A predicted pattern of energy vs detector location in the cislunar region is displayed for protons of zero pitch angle traveling upstream away from the quasi-parallel bow shock. The pattern is implied by upstream wave boundary properties deduced by Diodato et al. (1976). In the solar ecliptic, protons are estimated to have a minimum of 1.1 times the solar wind bulk energy E_{SW} when the wave boundary is in the early morning sector and a maximum of 8.2 E_{SW} when the boundary is near the predawn flank.

INTRODUCTION

At least some part of the cislunar solar wind region outside the earth's bow shock is continuously populated by particles and waves of shock or magnetospheric origin. The varying precursor region, or foreshock, is divided into several subregions, not all geometrically distinct, which are defined by differing particle species and wavemodes. One such subregion is characterized by the presence of backstreaming (herinafter called "return") protons of energy a few times the solar wind bulk flow energy and long-period, say 10 to 60-second, magnetic waves of amplitude about one-quarter of the magnitude of the upstream field $\underset{\sim}{B}_{SW}$. The return protons are thought to produce the waves (Fairfield, 1969; Greenstadt et al., 1970; Barnes, 1970; Fredricks, 1975), which are the more easily and commonly measured phenomenon, and the upstream, or sunward, boundary of this "proton-wave" foreshock is apparently well determined within contemporary experimental accuracy by a line tangent to the nominal bow shock cross section in the plane of X and $\underset{\sim}{B}_{SW}$ and at an angle to the solar ecliptic (SE) X-axis of $\theta_{XS} = \arctan [p \sin \theta_{XB}/(p \cos \theta_{XB} - 1)]$ (Greenstadt, 1974). In this expression, θ_{XB} is the angle between X and $\underset{\sim}{B}_{SW}$ and p represents a guiding-center velocity along $\underset{\sim}{B}_{SW}$ in the solar wind frame.

For the daylight portion of the shock, p averages about 2.0 overall, but appears from rough statistics to vary with the location of the tangent point, being about 1.6 in the subsolar region and rising above 2.0 toward the dawn and dusk flanks (Diodato et al., 1976).

A correlation between the occurrence of beams of return protons of specific energy and the appearance of long period upstream waves has not yet been established experimentally by direct observation of both phenomena simultaneously. Nor is such a correlation likely in the immediate future. Statistical study of return particle properties does seem quickly attainable, however, and one test of both of the particle-wave relationship and of the Diodato et al. dependence of p on inferred location of return proton origin would be to collect observations of return proton energies throughout the upstream region for many foreshock configurations. This note presents a first-order examination of the way in which the geometry of the foreshock wave boundary can be translated into a geometry of return proton energies.

A full characterization of foreshock particle and wave properties, including interactions with the incoming solar wind could be a complicated undertaking. Until at least an initial experimental survey is completed, it appears unpromising to attempt a full-scale description of all the observational results that could be inferred from a continuum of assumed pitch angles and production parameters. An appreciation of some problems associated with the latter can be obtained from an elementary study of the proton escape problem (Greenstadt, 1975). The following paragraphs offer an idealized example of return proton energies associated with the foreshock boundary and a discussion of several potential sources of complexity in nonideal experimental particle data.

IDEALIZED EXAMPLE

Detection Geometry. The relationship between various return particle velocity components and their observed energy E_r is shown in Figure 1. A beam of reflected bulk-velocity protons spirals up the field line with parallel and perpendicular velocities pV_{SW} and PV_{SW}, i.e., with pitch angle arctan (P/p), in the plasma frame, while being carried by the solar wind at velocity V_{SW}. The net return velocity V_r will define a direction along which a properly oriented, stationary particle detector will see the beam at energy $E_r=[p^2 + P^2 + 1-2(p \cos \theta_{XB} + P \cos \Omega_c t \sin \theta_{XB})] E_{SW}$ where Ω_c is the proton cyclotron period and E_{SW} is the energy associated with the solar wind bulk velocity (Greenstadt, 1975). We don't know how continuously a given spot A on the shock will produce a stream of p,P protons, so activation of the detector could be intermittent. It's obvious however that more than one combination of p and P can produce the same V_r, and some spectrum of return protons should be expected at most detector orientations. In the following example the perpendicular velocity contribution is neglected.

First order pattern. In Figure 2 the five segments of the dayside bow shock corresponding to the finest division described by Diodato et al. are shown symmetrically with respect to the solar ecliptic (SE) X-axis in an ecliptic-plane cross section. Connected to the nominal shock at each segment is an arc into which return protons would radiate outward from the shock with the appropriate velocity component pV_{SW} along $\underset{\sim}{B}_{SW}$ for the depicted range of $\underset{\sim}{B}_{SW}$ directions. The field is assumed to lie in the SE plane, and protons are indicated in terms of their zero-pitch angle (P=0) energy as it would

appear to a detector stationary in the earth frame and pointing into the direction from which the net return proton flux comes. What the picture tells us is that for $\underset{\sim}{B}_{SW}$ in the indicated direction ranges θ_{XB}, the foreshock wave boundary will lie in the corresponding sector subtended by the corresponding shock segment. Associated with the wave boundary in a given sector will be return protons of velocity $V_{||}$ and energy E_r appropriate to the same segment.

DISCUSSION

Foreshock boundary-protons will be neither unidirectional nor monoenergetic. There are four contributors to the spread in energies to be expected of ions coming from each segment. First, there ought to be the real pitch angle distribution represented by protons for which $P \neq 0$, and of course not all solar wind protons arrive at the shock with precisely the bulk velocity V_{SW} because of their thermal distribution.

Second, there may be a spectrum of p's produced at a given point of the shock even though only the ones found by Diodato et al. generate the waves.

Third, there is presumably a continuum of changing p values around the shock in three dimensions rather than averages over discrete zones in one plane as depicted. Time-changes in the nonecliptic Z-component of $\underset{\sim}{B}_{SW}$ and in the solar wind velocity direction, which aberrates the shock axis of symmetry, would tend to produce a mixture of particle energies in any given backstream direction over almost any finite time interval. Also, there is no reason developed yet that compels the dominant p to be rigidly

constant in time at a given point of the shock; local shock properties may affect the instantaneous value of p at any point.

Fourth, it seems likely that while the return protons coming from around the tangent point of the wave boundary at the shock have energies determined by the average p-relationship, protons coming from behind the foreshock boundary elsewhere on the quasi-parallel portion of the shock may be relased upstream with higher guiding center velocities, thus intersecting the boundary at varying distances from the shock. A hypothetical intersection of return particles from three points of the shock is illustrated in Figure 3. With the field at angle θ_{XB} so that the foreshock wave boundary is determined by p = 1.6 near the subsolar point, the figure postulates a property of the quasi-parallel shock in which p rises with decreasing θ_{nB} to a sharp maximum when $\theta_{nB} = 0$ (corresponding to parallel shock structure), focusing beams of particle guiding centers on cislunar observation point 0. The actual dependence of return particle energies on position of release along the shock or, more precisely, on θ_{nB}, for a given θ_{XB}, is still unmeasured, but it is known that 30 to 100 keV protons reach the moon's distance at about the same position as does the average foreshock boundary for $\theta_{XB} \approx 45°$ (Lin et al., 1974). The dashed lines continuing outward from 0 in Figure 3 call attention to the possibly complex pattern of the position-dependent particle population that may form the upstream signature for a given θ_{XB}.

For any θ_{XB}, protons coming from the shock along the foreshock boundary and responsible for the long-period foreshock waves should be distinguishable

from most others by their average direction of arrival. The important information in Figure 2 therefore is the trend in foreshock proton-guiding center energies that can be expected for different positions of the wave boundary, from the viewpoint of a suitably oriented detector. The anticipated trend includes a dip to minimal energies in the early to midmorning region of the foreshock and rather high energies near the western flank. The dip corresponds to the most probable interplanetary field orientations; the higher energies at the flank should be relatively unusual, since the responsible field directions are uncommon.

CONCLUSION

There is an idealized pattern of directions and energies of zero-pitch angle return protons traveling outward from the bow shock that can be inferred from the foreshock wave boundary results of Diodato et al. (1976). Suitably oriented satellite proton detectors should be able to test the association between upstream waves and backstreaming particles and the apparent p-dependence along the shock by seeking the expected pattern statistically. The results of such a test should serve as a guide to investigation of the more complex actual morphology of foreshock particles and ultimately to analysis of wave-particle interactions upstream and to return particle production and emission processes in the quasi-parallel shock.

ACKNOWLEDGMENT

This study was funded in part by NASA Contract NASW-2877 and in part by TRW Independent Research and Development.

REFERENCES

Barnes, A., Theory of generation of bow-shock-associated hydromagnetic waves in the upstream interplanetary medium, Cosmic Electrodyn., 1, 90, 1970.

Fairfield, D. H., Bow shock associated waves observed in the far upstream interplanetary medium, J. Geophys. Res., 74, 3541, 1969.

Fredricks, R. W., A model for generation of bow-shock-associated upstream waves, J. Geophys. Res., 80, 7, 1975.

Greenstadt, E. W., Structure of the terrestrial bow shock, Solar Wind Three, Proc. of the Third Solar Wind Conf., Asilomar, Ed. C. T. Russell, Inst. Geophys. & Planet. Phys., UCLA, 440, 1974.

Greenstadt, E. W., The upstream escape of energized solar wind protons from the bow shock, The Magnetospheres of Earth and Jupiter, Ed. V. Formisano, D. Reidel Pub. Co., Dordrecht, Holland, 3, 1975.

Greenstadt, E. W., I. M. Green, G. T. Inouye, D. S. Colburn, J. H. Binsack, and E. F. Lyon, Dual satellite observation of the earth's bow shock. 3. Field-determined shock structure, Cosmic Electrodyn., 1, 316, 1970.

FIGURE CAPTIONS

Figure 1. Geometry of return proton detection. A proton leaving the shock spirals around $\underset{\sim}{B}_{SW}$ at cyclotron frequency Ω_c in the solar wind, with velocity $\underset{\sim}{V}_p$ having parallel and perpendicular components $\underset{\sim}{V}_{\parallel}$ and $\underset{\sim}{V}_{\perp}$. A suitably-oriented detector, stationary with respect to the earth, sees the proton with net return energy E_r after the solar wind velocity $\underset{\sim}{V}_{SW}$ has been added to $\underset{\sim}{V}_p$ to make final return velocity $\underset{\sim}{V}_r = \underset{\sim}{V}_p + \underset{\sim}{V}_{SW}$. The expression for $\underset{\sim}{V}_r$ is based on defining $\underset{\sim}{P}_1$ in the plane of $\underset{\sim}{B}_{SW}$ and X (i.e., $\underset{\sim}{B}_{SW}$ and $\underset{\sim}{V}_{SW}$) and perpendicular to $\underset{\sim}{B}_{SW}$, and $\underset{\sim}{P}_2 = \underset{\sim}{P}_1 \times \underset{\sim}{B}_{SW}$. Angle θ_{XB} is between X (i.e., $-\underset{\sim}{V}_{SW}$) and $\underset{\sim}{B}_{SW}$.

Figure 2. Pattern of zero pitch-angle, return particle energy ranges for protons at the leading edge of the foreshock in five shock sectors determined by orientation of $\underset{\sim}{B}_{SW}$ in the ecliptic plane. The directions of $\underset{\sim}{B}_{SW}$ (arrows) and ranges of θ_{XB} which place the foreshock boundary in the various sectors are shown in the small insert frames. The pairs of numbers at the top of each sector give the average p over the sector (upper number) and the corresponding range of return energy E_r (lower number).

Figure 3. Hypothetical example of a possible cislunar convergence of return protons of mixed energies. For a fixed $\underset{\sim}{B}_{SW}$ (in the ecliptic) the local value of p, indicated at three locations along the inside of the shock, could increase dramatically with the local approach to parallel structure, i.e., $\underset{\sim}{B}_{SW}$ parallel to the local normal $\underset{\sim}{n}$.

Figure 3. (Cont'd)

Fast protons with p = 10 could arrive from the flank at the same observation point $\underset{\sim}{0}$ as slower protons with p = 1.6 arrive from the subsolar region.

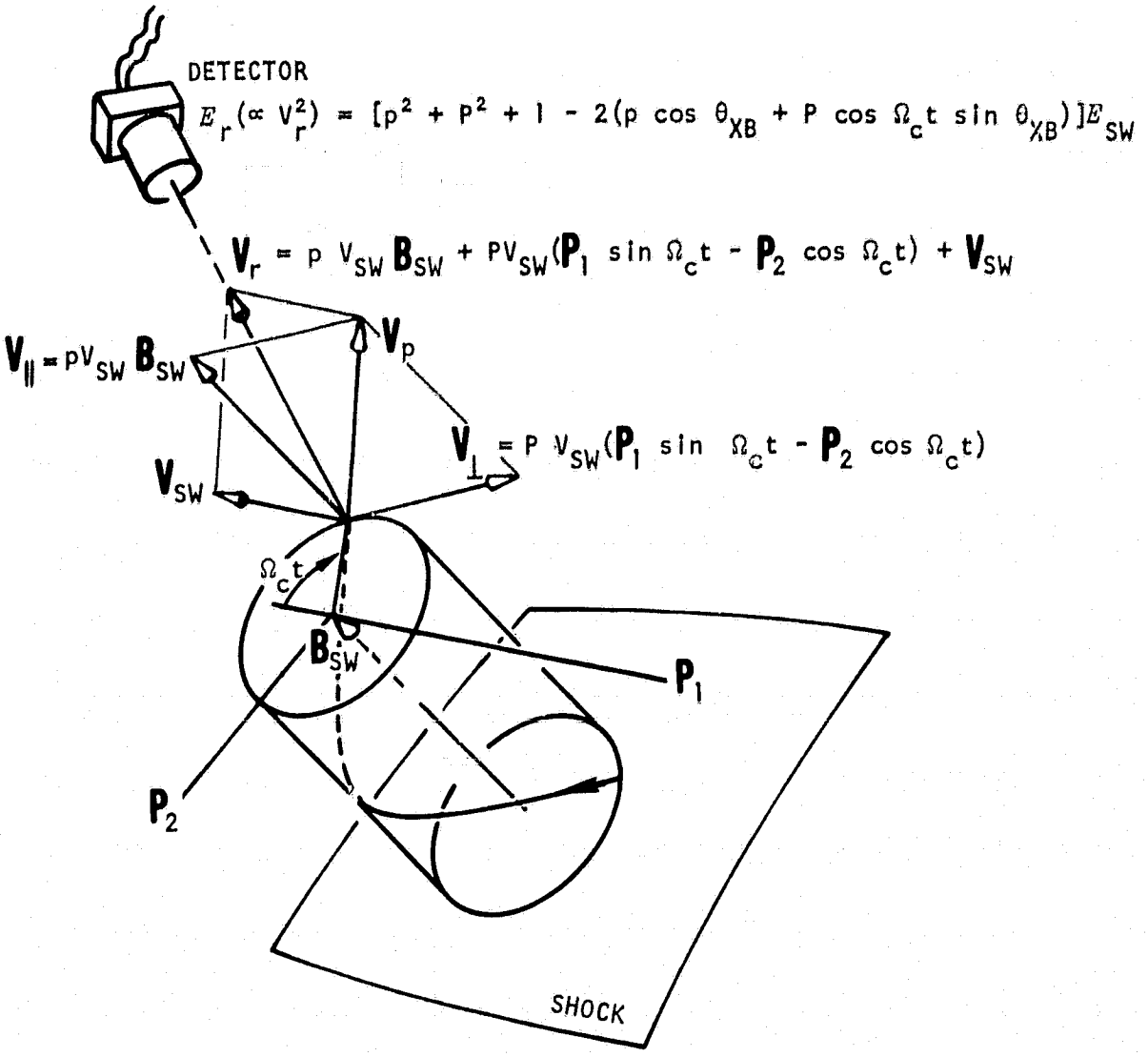

Figure 1. Geometry of return proton detection. A proton leaving the shock spirals around $\underset{\sim}{B}_{SW}$ at cyclotron frequency Ω_c in the solar wind, with velocity $\underset{\sim}{V}_p$ having parallel and perpendicular components $\underset{\sim}{V}_{\parallel}$ and $\underset{\sim}{V}_{\perp}$. A suitably-oriented detector, stationary with respect to the earth, sees the proton with net return energy E_r after the solar wind velocity $\underset{\sim}{V}_{SW}$ has been added to $\underset{\sim}{V}_p$ to make final return velocity $\underset{\sim}{V}_r = \underset{\sim}{V}_p + \underset{\sim}{V}_{SW}$. The expression for $\underset{\sim}{V}_r$ is based on defining $\underset{\sim}{P}_1$ in the plane of $\underset{\sim}{B}_{SW}$ and X (i.e., $\underset{\sim}{B}_{SW}$ and $\underset{\sim}{V}_{SW}$) and perpendicular to $\underset{\sim}{B}_{SW}$, and $\underset{\sim}{P}_2 = \underset{\sim}{P}_1 \times \underset{\sim}{B}_{SW}$. Angle θ_{XB} is between X (i.e., $-\underset{\sim}{V}_{SW}$) and $\underset{\sim}{B}_{SW}$.

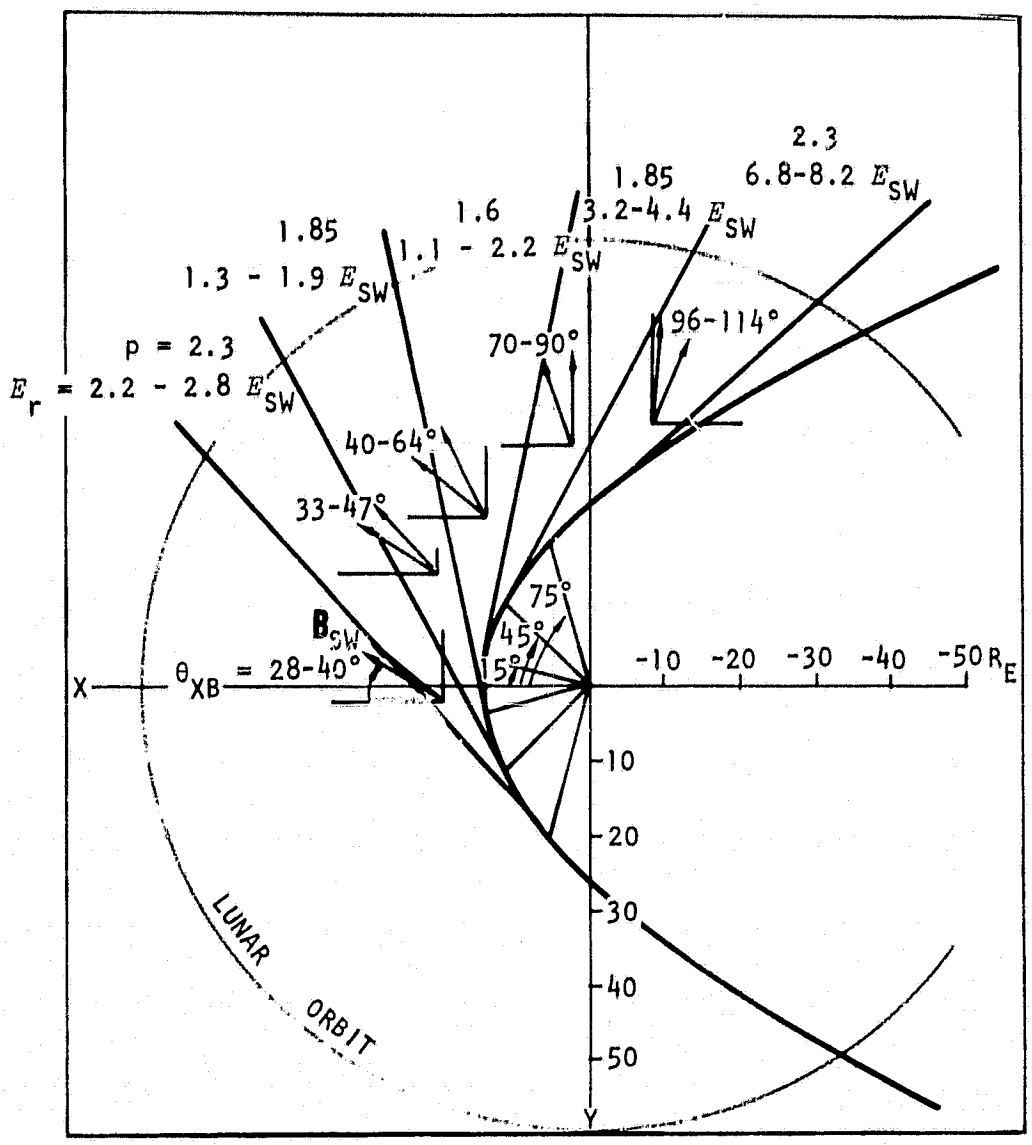

Figure 2. Pattern of zero pitch-angle, return particle energy ranges for protons at the leading edge of the foreshock in five shock sectors determined by orientation of $\underset{\sim}{B}_{SW}$ in the ecliptic plane. The directions of $\underset{\sim}{B}_{SW}$ (arrows) and ranges of θ_{XB} which place the foreshock boundary in the various sectors are shown in the small insert frames. The pairs of numbers at the top of each sector give the average p over the sector (upper number) and the corresponding range of return energy E_r (lower number).

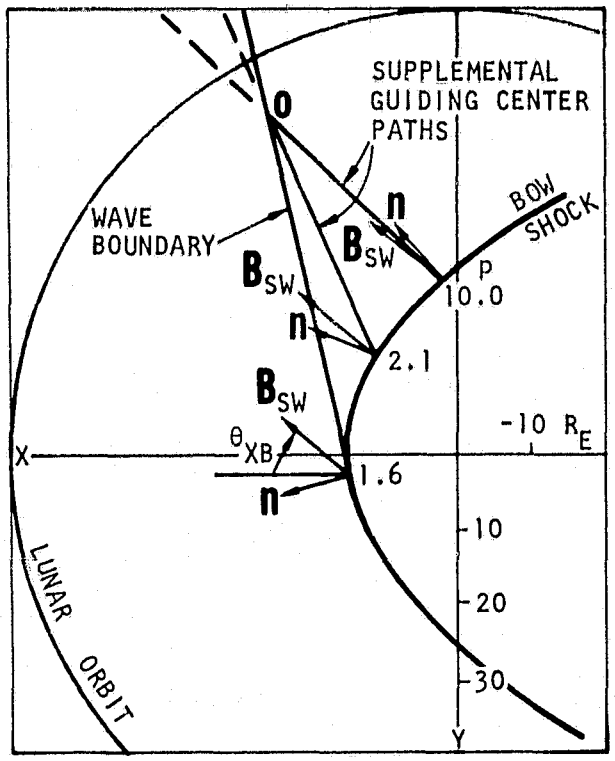

Figure 3. Hypothetical example of a possible cislunar convergence of return protons of mixed energies. For a fixed $\underset{\sim}{B}_{SW}$ (in the ecliptic) the local value of p, indicated at three locations along the inside of the shock, could increase dramatically with the local approach to parallel structure, i.e., $\underset{\sim}{B}_{SW}$ parallel to the local normal $\underset{\sim}{n}$. Fast protons with p = 10 could arrive from the flank at the same observation point $\underset{\sim}{O}$ as slower protons with p = 1.6 arrive from the subsolar region.